

Direct Numerical Simulation of Particle-Laden Homogeneous Isotropic Turbulent Flows Using a Two-Fluid Model Formulation

André Kaufmann¹, Olivier Simonin², Thierry Poinsot³

1 : CERFACS, Toulouse, France, kaufmann@cerfacs.fr*

2,3 : IMFT, UMR 5502 CNRS/INPT/UPS, Toulouse, France, simonin@imft.fr, poinsot@imft.fr

Abstract A DNS approach for Eulerian-Eulerian dispersed particles simulation is presented in which a stress term corresponding to the uncorrelated motion of dispersed particles is identified. Two models for this stress terms are proposed. The first model uses an isentropic approximation that relates the local amount of uncorrelated particle kinetic energy to the particle number density. The second model uses a transport equation comparable to the transport equation for the internal energy in the Navier Stokes equations. The validity of the Eulerian-Euler formulation is discussed by comparing to a Lagrangian particle tracking simulation using identical carrier phase realisation. It is found that the dispersed phase behaves in both simulations like a very compressible gas when the Stokes number is close to unity. The resulting strong gradients in the particle number density field can not be resolved on the grid which is sufficient for DNS of the carrier phase. Spectral analysis of the correlated particle velocity shows the limits of validity of the present simulations.

1 Introduction

Numerical Simulations coupling Lagrangian tracking of discrete particles with DNS (or LES) of the carrier-phase turbulence provide a well established powerful tool to investigate particle laden flows, but such numerical simulations have the drawback of being numerically very expensive for practical applications. Numerical simulations based on separate Eulerian balance equations for both phases, coupled through inter-phase exchange terms, might be an effective alternative approach. Such Euler-Euler (or two-fluid) DNS approach has been validated for the case of particles with very low inertia which follow the carrier fluid flow almost instantaneously due to their small response time compared to the time microscales of the turbulence[2].

But as shown by Février [6], in the case of inertial particles with response times larger than the Kolmogorov time scale, the Eulerian approach for the dispersed phase must account specifically for the effects due to a random part of the particle velocities which is not spatially correlated (or which satisfies the “molecular chaos assumption”). Following Février et al. [7] the conditional average of the particle properties with respect to the same carrier phase turbulent flow realization allows the derivation of instantaneous Eulerian transport equations, governing the spatially correlated part of the particle velocities, from a kinetic equation of a conditional particle pdf. From numerical simulations coupling Lagrangian particle tracking of discrete particles with DNS of forced isotropic turbulence, Février [6] showed that the uncorrelated part of the particle velocities increases with inertia. In case such that, when the particle relaxation time is comparable to the fluid Lagrangian integral time scale, the uncorrelated kinetic energy is about 30% of the total kinetic energy of the particles.

The general purpose of this presentation¹ is the application of such an Euler-Euler DNS approach for the computation of a decaying gas-particle homogeneous isotropic turbulence with one-way coupling. Two-phase flow simulations for the same conditions have been performed on structured meshes with 64^3 , 128^3 and 192^3 grid points. Analysis of the numerical results show that the standard Euler-Euler model does well in the tracer limit, as expected. In contrast, for inertial particles, the need for explicit

*present address: Siemens VDO, Regensburg Germany, Andre.Kaufmann@siemens.com

pressure and stress terms accounting for the effect of the uncorrelated part of the particle velocities in the dispersed phase momentum equation is clearly identified. Models for such terms are tested and classified. Inertial particle simulation results are found to be very sensitive to the mesh refinement when the particle relaxation time is greater or equal to roughly 1/10 of the turbulent time macroscale because the smallest length scales of the predicted dispersed phase velocity field can become significantly smaller than the smallest length scales of the carrier phase turbulent motion.

The Euler-Euler DNS approach is finally validated by a direct comparison of the predictions (particle number density and correlated velocity fields, correlated and uncorrelated kinetic energies, spectral correlated energy distribution) with results from numerical simulations coupling Lagrangian particle tracking of about 10^7 discrete particles with the DNS of the identical carrier turbulent flow computed on a mesh with 64^3 grid points.

2 The Eulerian model

Eulerian equations for the dispersed phase may be derived by several means. A popular simple way consists of volume filtering of the the separate, local, instantaneous phase equations accounting for the inter-facial jump conditions [3]. Such an averaging approach is very restrictive, because particle sizes and particle distances have to be smaller than the smallest length scale of the turbulence.

A different, not totally equivalent way is the statistical approach in the framework of kinetic theory. In analogy to the derivation of the Navier-Stokes equations by kinetic theory [1], a probability density function (pdf) $f_p^{(1)}(\mathbf{c}_p; \mathbf{x}_p, t)$ may be defined. This gives the local instantaneous probable number of particles with the given translation velocity $\mathbf{u}_p = \mathbf{c}_p$. This function obeys a Boltzmann-type kinetic equation, which accounts for momentum exchange with the carrier fluid and for the influence of external forces such as gravity and inter-particle collisions. Transport equations of the first moments (such as particle concentration, mean velocity and particle kinetic stress) may be derived directly by averaging from the pdf kinetic equation [15].

For the sake of simplicity in this feasibility study, interaction forces are limited to drag, considering non-evaporating particles in absence of gravity. The extension to evaporating flows, gravity force, turbulence corrections in the drag force and other interaction forces is not in conflict with the presented derivation of the Eulerian field equations. In the presented approach the gas is presumed undisturbed by the dispersed phase. Therefore the passage from one-way to two-way coupling is more delicate.

2.1 Conservation Equations for particle properties

To derive local instantaneous Eulerian equations in dilute flows (without turbulence modification by the particles), Février et al. [7], [6], [16] propose to use an averaging over all dispersed-phase realizations conditioned by one carrier-phase realization. Such an averaging procedure leads to a conditional velocity pdf for the dispersed phase,

$$\check{f}_p^{(1)}(\mathbf{c}_p; \mathbf{x}, t, H_f) = \langle W_p^{(1)}(\mathbf{c}_p; \mathbf{x}, t) | H_f \rangle. \quad (1)$$

$W_p^{(1)}$ are the realizations of position and velocity in time of any given particle [14] and H_f is the unique carrier flow realization. With this definition one may define a local instantaneous particulate velocity field, which is here named ‘‘mesoscopic Eulerian particle velocity field’’. This field is obtained by averaging the conditioned velocity pdf over all particle-flow realizations.

$$\check{u}_p(\mathbf{x}, t, H_f) = \frac{1}{\check{n}_p} \int \mathbf{c}_p \check{f}_p^{(1)}(\mathbf{c}_p; \mathbf{x}, t, H_f) d\mathbf{c}_p. \quad (2)$$

Here

$$\check{n}_p = \int \check{f}_p^{(1)}(\mathbf{c}_p; \mathbf{x}, t, H_f) d\mathbf{c}_p \quad (3)$$

is the “mesoscopic” particle-number density and

$$\langle \check{\Phi} \rangle_p = \frac{1}{\check{n}_p^{(1)}} \int \check{f}_p^{(1)} \Phi d\mathbf{c}_p \quad (4)$$

stands for any ensemble averaged quantity.

For simplicity, the dependence of the above variables on H_f is not shown explicitly. Application of the conditional-averaging procedure to the kinetic equation governing the particle pdf leads directly to the transport equations for the first moments of number density and mesoscopic Eulerian velocity,

$$\frac{\partial}{\partial t} \check{n}_p + \frac{\partial}{\partial x_i} \check{n}_p \check{u}_{p,i} = 0 \quad (5)$$

$$\check{n}_p \frac{\partial}{\partial t} \check{u}_{p,i} + \check{n}_p \check{u}_{p,j} \frac{\partial}{\partial x_j} \check{u}_{p,i} = -\frac{\check{n}_p}{\tau_p} [\check{u}_{p,i} - u_i] - \frac{\partial}{\partial x_j} \check{n}_p \delta \check{\sigma}_{p,ij} \quad (6)$$

Here $\delta \check{\sigma}_{p,ij}$ is the mesoscopic kinetic stress tensor of the particle velocity distribution discussed in section 2.2. One of the current objectives is to show that this term is non-negligible for inertial particles in turbulent flow. Due to the very small droplet Reynolds number value measured in the simulation, the particle relaxation time τ_p is defined as the relaxation time for Stokes drag.

$$\tau_p = \frac{\rho_p d^2}{18\mu} \quad (7)$$

2.2 The stress tensor of Random Uncorrelated Motion (RUM)

The stress term in eq. 6 arises from an ensemble average of the nonlinear term in the transport equation for particle momentum,

$$\check{n}_p \delta \check{\sigma}_{p,ij} = \int (c_{p,i} - \check{u}_{p,i}) (c_{p,j} - \check{u}_{p,j}) \check{f}_p^{(1)}(\mathbf{c}_p; \mathbf{x}, t, H_f) d\mathbf{c}_p \quad (8)$$

$$= \check{n}_p \langle \delta u_{p,i} \delta u_{p,j} | H_f \rangle_p. \quad (9)$$

and contains the uncorrelated part of the particle motion. The uncorrelated part of the particle velocity is here referred to as Random Uncorrelated Motion (RUM) ¹ When the Euler or Navier-Stokes equations are derived from kinetic gas theory the trace of $\langle \delta u_{p,i} \delta u_{p,j} \rangle_p$ is interpreted as temperature (ignoring the Boltzmann constant and molecular mass) and related to pressure by an equation of state. In the case of the Euler or Navier-Stokes equations temperature is defined as the uncorrelated part of the kinetic energy. Here the uncorrelated part of the particulate kinetic energy is defined as

$$\delta \check{\theta}_p = \frac{1}{2} \langle \delta u_{p,i} \delta u_{p,i} | H_f \rangle_p. \quad (10)$$

In analogy to the Euler or Navier-Stokes equations a Random Uncorrelated Motion Pressure (RUMP) may be defined by the product of uncorrelated kinetic energy and particle number density, as

$$P_{RUM} = \check{n}_p \frac{2}{3} \delta \check{\theta}_p \quad (11)$$

When the particle number distribution becomes nonuniform, as in the case of a compressible gas, this pressure term tends to homogenize particle number density.

¹Random Uncorrelated Motion (RUM) has been referred to as *Quasi Brownian Motion (QBM)* in previous publications. We agree that the expression *Quasi Brownian* is misleading since the physical interpretation of the uncorrelated motion is not of *brownian* nature.

The non-diagonal elements of the stress tensor can be identified, in analogy to the Navier-Stokes equations, as a viscous terms due to shear. The diagonal part of the stress tensor is then proportional to one third of the trace of the tensor and an eventual deviation such that ($\check{n}_p \delta \check{\sigma}_{p,ij} = P_{RUM} \delta_{ij} - \delta \check{\tau}_{p,ij}$). The momentum-transport equation (6) becomes

$$\check{n}_p \frac{\partial}{\partial t} \check{u}_{p,i} + \check{n}_p \check{u}_{p,j} \frac{\partial}{\partial x_j} \check{u}_{p,i} = -\frac{\check{n}_p}{\tau_p} [\check{u}_{p,i} - \check{u}_{f,i}] - \frac{\partial}{\partial x_i} P_{RUM} + \frac{\partial}{\partial x_j} \delta \check{\tau}_{p,ij} \quad (12)$$

In analogy to the derivation of the Navier-Stokes equations from kinetic gas theory the stress term can be related to the gradients of the first moments based on the Onsager relations [8]. Making some assumptions on symmetry and isotropy the stress term can be modeled as detailed below:

$$\delta \check{\tau}_{p,ij} = \mu_{RUM} \left(\frac{\partial \check{u}_{p,i}}{\partial x_j} + \frac{\partial \check{u}_{p,j}}{\partial x_i} - \frac{2}{3} \frac{\partial \check{u}_{p,k}}{\partial x_k} \delta_{ij} \right) \quad (13)$$

The dynamic viscosity related to Random Uncorrelated Motion can be estimated by $\mu_{RUM} = 1/3 \check{n}_p \tau_p \delta \check{\theta}_p$ [16] where τ_p is the relaxation time related to Stokes drag. This expression can be obtained using the transport equation for the separate stresses $\langle \delta u_{p,i} \delta u_{p,j} \rangle$ and supposing weak shear [1].

Preliminary tests with the closure model given in eq.13 failed since large segregation effects around unity Stokes number imply shock like strong number density gradients that could not be handled by the numeric scheme [9]. There are two possible origins of this difficulty: the chosen spatial resolution is insufficient to resolve the physics or the closure model does not describe the proper physics. Supposing that the numerical resolution of the model is insufficient, several possibilities exist to circumvent this difficulty. A different numerical scheme using up-winding or flux limiters would clearly be able to capture those strong gradients but imply some type of numerical diffusion. Increasing spatial resolution increases strongly numerical cost such that here a filtering approach by a *subgrid* model acting on the compressible component of the velocity is chosen. This subgrid model has the form of a bulk viscous term $\xi_{SGS} \partial \check{u}_k / \partial x_k \delta_{ij}$ which is added to the shear viscosity term $\delta \check{\tau}_{p,ij}$ in eq.13. The subgrid bulk viscosity is mesh-size dependent ($\xi_{SGS} \propto \check{n}_p (\Delta x)^2 |\partial \check{u}_k / \partial x_k|$). In homogeneous turbulence, the spatial average of this bulk viscous term is zero, still it acts locally and leads to a smoothing of the number density field. Computations are performed with this heuristically introduced bulk viscosity.

The closure model (eq. 13) requires the knowledge of $\delta \check{\theta}_p$ which is developed in the next section.

2.3 The equation for Random Uncorrelated kinetic Energy (RUE)

To calculate the RUE, two approaches are presented; the first one assumes a quasi isentropic behavior of the dispersed phase leading to an algebraic expression for $\delta \check{\theta}_p$.

$$\delta \check{\theta}_p = A \check{n}_p^{2/3} \quad (14)$$

A is the residual mean kinetic energy of the particles averaged over the computational domain weighted by moments of the particle distribution. In order to define A it is necessary to introduce some definitions. Spatial averages (over the computational domain) are defined by $\{\phi\} = 1/V \int_V \phi dV$. Particle pondered averages are defined by $\{\phi\}_p = \{\check{n}_p \phi\} / \{\check{n}_p\}$. This allows to define $A = \{\check{n}_p\} \delta q_p^2 / \{\check{n}_p^{5/3}\}$. The mean residual particle kinetic energy is defined as $\delta q_p^2 = \{\delta \check{\theta}_p\}_p$. The expression in eq. 14 relates therefore the local residual particle kinetic energy to the mean residual particle kinetic energy. It can be obtained using the conservation equation for number density (eq. 5) and the lowest order conservation equation for Random Uncorrelated Energy (RUE) in the Chapman-Enskog expansion [1]:

$$\frac{\partial}{\partial t} \check{n}_p \delta \check{\theta}_p + \frac{\partial}{\partial x_j} \check{n}_p \check{u}_{p,j} \delta \check{\theta}_p = -\frac{2}{3} \check{n}_p \delta \check{\theta}_p \frac{\partial \check{u}_{p,j}}{\partial x_j} \quad (15)$$

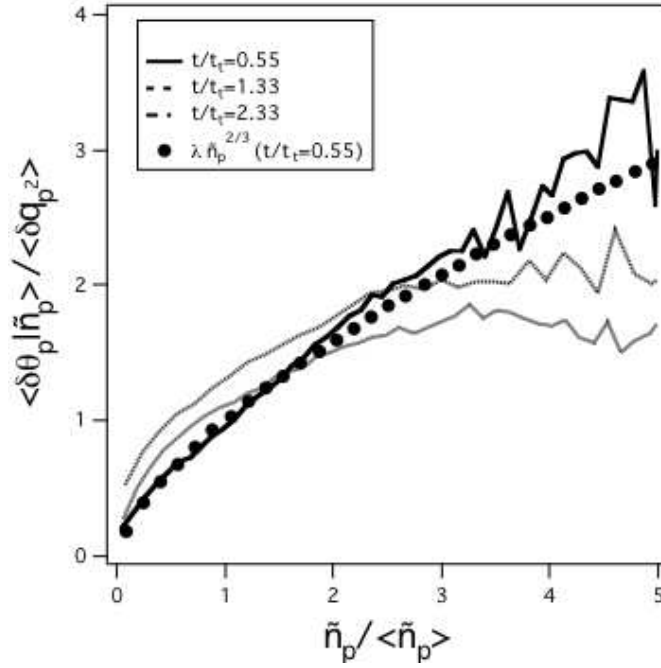


Figure 1: Conditional average of RUM Energy on the number density in the Lagrangian computation at different times.

It is then sufficient to multiply eq. 5 by $-\frac{2}{3}\tilde{n}_p^{-5/3}\delta\check{\theta}_p$ and to add the resulting expression to eq. 15 times $\tilde{n}_p^{-2/3}$ to achieve a transport equation for $\tilde{n}_p^{-2/3}\delta\check{\theta}_p$ with a zero right hand side. Lagrangian simulations performed by P. Février [6] in stationary homogeneous isotropic turbulence suggest that the mean residual kinetic energy δq_p^2 depends on the resolved dispersed phase kinetic energy $\check{q}_p^2 = 1/2 \{ \check{u}_{p,k} \check{u}_{p,k} \}_p$, the fluid-particle correlation $q_{fp} = \{ \check{u}_{p,k} u_k \}_p$ where u_k is the carrier phase velocity, and the carrier phase kinetic energy pondered by the particle presence $q_{f@p}^2 = 1/2 \{ u_k u_k \}_p$. This expression is given by

$$\delta q_p^2 = \check{q}_p^2 \left(\frac{4\check{q}_p^2 q_{f@p}^2}{q_{fp}^2} - 1 \right) \quad (16)$$

The second approach uses the full transport equation for random uncorrelated kinetic energy [16]:

$$\begin{aligned} \frac{\partial}{\partial t} \tilde{n}_p \delta\check{\theta}_p + \frac{\partial}{\partial x_j} \tilde{n}_p \check{u}_{p,j} \delta\check{\theta}_p = & -2 \frac{\tilde{n}_p}{\tau_p} \delta\check{\theta}_p \\ & - \left[P_{RUM} \delta_{ij} - \xi_{SGS} \frac{\partial \check{u}_{p,k}}{\partial x_k} \delta_{ij} - \mu_{RUM} \left(\frac{\partial \check{u}_{p,i}}{\partial x_j} + \frac{\partial \check{u}_{p,j}}{\partial x_i} - \frac{2}{3} \frac{\partial \check{u}_{p,k}}{\partial x_k} \delta_{ij} \right) \right] \frac{\partial \check{u}_{p,i}}{\partial x_j} \\ & + \frac{\partial}{\partial x_j} \left[k_{RUM} \frac{\partial}{\partial x_j} \delta\check{\theta}_p \right] \end{aligned} \quad (17)$$

This equation is the equivalent of the internal energy equation in the Navier Stokes equation. It contains the same mechanisms such as increase in internal energy due to compression, production by shear the modeling of the third order correlation by a diffusive flux. The diffusivity constant for RUM is estimated by $k_{RUM} = 5/3 \tilde{n}_p \tau_p \delta\check{\theta}_p$. This is the equivalent of the Fick's law for the heat flux in the Navier-Stokes equations. The only additional term in eq. 17 is due to drag since the uncorrelated motion is dissipated by the drag friction with the carrier phase.

3 Description of the numerical test case

Homogeneous isotropic turbulence is one of the classical cases where dynamics and dispersion of particle laden flows can be studied. This has been done extensively using the Lagrangian formalism and encouraging results and insight are obtained by such methods. Comparison of Lagrangian particle tracking in decaying homogeneous isotropic turbulence [4] with experimental measurements of particle dispersion in grid generated turbulence [17] show that essential features of the particle dynamics can be captured. Preliminary computations with a simplified Eulerian formalism of this test case gave encouraging results [10]. In the case of tracer particles (small Stokes number limit) Eulerian methods are well suited to describe the dynamics [3]. With increasing Stokes number the particle velocities become de-correlated from the gaseous carrier phase velocity. Inertia effects become important and segregation occurs for Stokes numbers about unity. The subject of the study is therefore not only the development of an adequate numerical tool but the validity of the Eulerian approach for Stokes numbers from the tracer limit ($St \rightarrow 0$) to unity. For the sake of simplicity here the case of decaying homogeneous isotropic turbulence is studied. The carrier phase is initially supposed to have uniform density and the velocity field to be divergence free and the kinetic energy to follow a Passot-Pouquet spectrum [13]. After roughly one turn over time the velocity field is supposed a true solution of the Navier Stokes equations and the dispersed phase is initialized. In the Lagrangian reference simulation particles are homogeneously distributed in space and the initial particle velocities are equal to the carrier phase velocity at the location of the particle. For the Eulerian computation this corresponds to homogeneous particle number density field and a mesoscopic particle velocity equal to the carrier phase velocity. RUM is zero for this initialization and should develop during the simulation.

4 Computation of the Lagrangian reference solution

The Lagrangian particle tracking method is a well understood tool for the numerical investigation of particle laden turbulence. In the case of Stokes drag the particle coordinate and velocities are advanced in time with the following set of differential equations.

$$\frac{\partial}{\partial t} X_i^{(k)} = V_i^{(k)} \quad (18)$$

$$\frac{\partial}{\partial t} V_i^{(k)} = \frac{1}{\tau_p} \left(u_i(X_i^{(k)}, t) - V_i^{(k)} \right) \quad (19)$$

In realistic applications particle numbers are so large that it is not possible to track all particles individually and particles are advanced as “numerical” particles that are supposed to represent a large number of “physical” particles. In order not to bias the result by such a procedure here all particles are computed individually. Special care is taken to evaluate the gaseous velocity u_i at the particle location for the drag force by using high order interpolation methods [19]. The spatial resolution of the gaseous phase is 64^3 and an average of 40 particles are computed per gaseous node. This corresponds to a total of 10.48 million individual particles. This high particle number ensures convergence when grid filtered fields are computed from the discrete particle distribution. The resulting continuous fields are sensitive to the numerical procedure used. With the high number of particles used the error can be shown to be smaller than 3%. This error has been estimated by using different filtering methods on the carrier phase grid.

The carrier phase is solved by a 6th order spatial scheme with Runge Kutta time stepping. For the evaluation of drag force, the velocity of the carrier phase is computed at the particle location using interpolation methods.

5 Spectral properties

Using the Fourier transformed velocities of the carrier phase $\hat{u}_i(k) = \mathcal{F}(u_i(x))$ and dispersed phase $\hat{u}_{p,i}(k) = \mathcal{F}(\check{u}_{p,i}(x))$ one can construct three dimensional energy spectra and a spectral fluid-particle correlation.

$$E_f(k) = \frac{1}{2} \hat{u}_i(k) \hat{u}_i(k) \quad (20)$$

$$E_p(k) = \frac{1}{2} \hat{u}_{p,i}(k) \hat{u}_{p,i}(k) \quad (21)$$

$$E_{fp}(k) = \hat{u}_i(k) \hat{u}_{p,i}(k) \quad (22)$$

For established turbulent flow the undisturbed carrier phase kinetic energy follows the famous Kolmogorov spectrum. Here the interest lies on the behavior of the spectrum of the correlated particle kinetic energy and the fluid-particle correlation. Whereas the carrier phase is considered incompressible segregation effects show that there must be a compressible component to the correlated dispersed phase velocity. With the definition of Kraichnan [12] operators in the spectral velocity can be divided into a compressible and an incompressible (solenoidal) component.

$$\hat{u}_{p,i}^c = \frac{\kappa_i \kappa_j}{\kappa^2} \hat{u}_{p,j} \quad (23)$$

$$\hat{u}_{p,i}^s = \left(1 - \frac{\kappa_i \kappa_j}{\kappa^2}\right) \hat{u}_{p,j} \quad (24)$$

$$(25)$$

This orthogonal decomposition allows to construct a compressible and a solenoidal spectral energy such that the sum equals to the total spectral energy.

$$E_p^c(k) = \frac{1}{2} \hat{u}_{p,i}^c(k) \hat{u}_{p,i}^c(k) \quad (26)$$

$$E_p^s(k) = \frac{1}{2} \hat{u}_{p,i}^s(k) \hat{u}_{p,i}^s(k) \quad (27)$$

Compressible kinetic energy is a phenomena that occurs in also supersonic turbulence such as in interstellar gases that are highly compressible.

6 Reconstruction of the filter kernel

Here it is assumed that $\bar{\check{n}}_p$ is the filtered number density field of the equivalent resolved number density field \check{n}_p . Formally the filtered number density field is obtained by the following convolution with the filter kernel:

$$\bar{\check{n}}_p(x) = \int \check{n}_p(x') F(x' - x) dx' \quad (28)$$

Using the Fourier transform property the convolution becomes a product in spectral space:

$$\hat{\bar{\check{n}}}_p(\boldsymbol{\kappa}) = \hat{\check{n}}_p(\boldsymbol{\kappa}) \hat{F}(\boldsymbol{\kappa}) \quad (29)$$

Finally, by the real space filter kernel can be obtained by backward Fourier transform:

$$F(x) = \mathcal{F}^{-1} \left(\frac{\hat{\bar{\check{n}}}_p(\boldsymbol{\kappa})}{\hat{\check{n}}_p(\boldsymbol{\kappa})} \right) \quad (30)$$

The filtering kernel allows a qualitative comparison of the particle number density field obtained by the grid filtering of the Lagrangian simulation and the Eulerian prediction of the particle number density field. When favre averaging is assumed this allows further more to obtain the filtered quantities of mesoscopic velocity and RUM that correspond to the Eulerian prediction with subgrid operator.

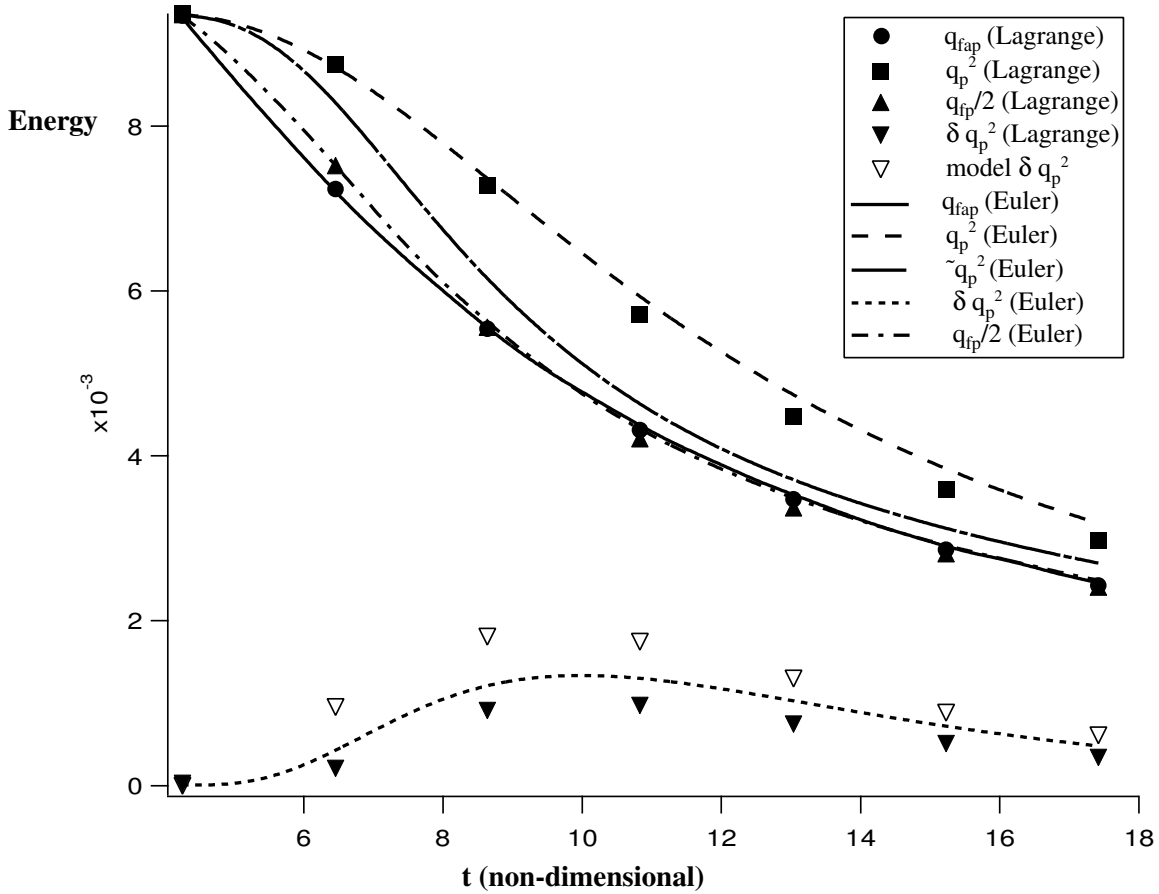


Figure 2: Temporal evolution of the fluid, particle and fluid-particle velocity correlations in an homogeneous isotropic decaying two-phase turbulence, comparison of results from Lagrangian simulations (symbols) and Eulerian simulations (lines). For Eulerian-Eulerian approach the total particle kinetic energy q_p^2 is computed as the sum of the kinetic energy due to correlated motion \tilde{q}_p^2 and the random uncorrelated energy δq_p^2 .

7 Results and Discussion

The Eulerian simulation is performed using a different code from the Lagrangian reference solution. It uses a second order spatial scheme with a second order temporal correction (Lax Wendroff). For the test cases carrier phase solutions are identical and velocity spectra superpose. The dispersed phase is computed using the same numerical method as the carrier phase imposing an additional limit on the time step due to particle relaxation time. Simulations have been carried out for several particle relaxation times.

7.1 Temporal evolution

In Fig. 2 the temporal evolution of carrier phase kinetic energy, particle kinetic energy and fluid-particle correlation are shown. The properties are averaged over the computational volume and defined for the Eulerian simulation by

$$q_f^2 = \frac{1}{V} \int \frac{1}{2} u_k u_k dV \quad (31)$$

$$q_{fp}^2 = \frac{1}{V} \int \check{u}_{p,k} u_k dV \quad (32)$$

$$\check{q}_p^2 = \frac{1}{V} \int \frac{1}{2} \check{u}_{p,k} \check{u}_{p,k} dV \quad (33)$$

and for the Lagrangian simulation by

$$q_{fp}^2 = \frac{1}{N} \sum_i V_k^{(i)} u_k \quad (34)$$

$$q_p^2 = \frac{1}{N} \sum_i \frac{1}{2} V_k^{(i)} V_k^{(i)} \quad (35)$$

The energy due to uncorrelated motion (RUE) is defined by

$$\delta q_p^2 = \frac{1}{N} \sum_i \frac{1}{2} (V_k^{(i)} - \check{u}_{p,k})(V_k^{(i)} - \check{u}_{p,k}) \quad (36)$$

such that the total particle kinetic energy can be decomposed $q_p^2 = \check{q}_p^2 + \delta q_p^2$.

The carrier phase kinetic energy decreases due to viscosity. Particle kinetic energy follows the carrier phase kinetic energy with a delay of the order of the particle relaxation time. Due to particle inertia, the particle velocities become partially uncorrelated in space and RUE begins to increase. This behavior of the integral quantities of correlated and uncorrelated particle kinetic energy as well as the fluid-particle correlation are well predicted by the Eulerian simulation using the transport equation for RUE. Simulations using the isentropic approximation show results of similar quality.

7.2 Instantaneous local fields

Fig. 3 shows snapshots of number density and RUM Energy in the Lagrangian and the Eulerian computation. The number density in the Eulerian computation admits smaller variations than the number density in the Lagrangian computation due to the heuristically introduced bulk viscosity. This bulk viscosity acts on the compressible component of the velocity and thus limits compressibility effects. Random Uncorrelated Energy admits qualitatively the same structures in the Eulerian and Lagrangian computation.

The heuristically introduced bulk viscous term tends to render the spatial particle number density more uniform. Without this bulk viscous term calculations can currently not be carried out: the physical particle segregation is too large as it could be resolved by the numerical scheme. Since the spatial average of the volume viscosity is however zero, it does not effect the temporal evolution of the averaged kinetic energy of Random Uncorrelated Motion of the particles δq_p^2 . Local values instantaneous values of $\delta \check{\theta}_p$ may differ notably from the values obtained in the Lagrangian simulation. An important remaining question is therefore attached to the subgrid model in form of a bulk viscous term. Higher spatial resolutions should clarify this problem if the encountered difficulties are related to numerical resolution. It is however not clear if the modeling of stresses by eq. 13 represents correctly the physics and if this is at the origin of the encountered difficulties. This point is under current investigation with the strong support of the Lagrangian simulations.

7.3 Spectral kinetic energies

Fig. 4 shows spectra of the total kinetic energies of the dispersed phase as well as the compressible kinetic energies of the Lagrangian and the Eulerian computation. First one remarks the high compressible component of the kinetic energy compared to the gaseous carrier phase kinetic energy. This causes structures similar to those known as eddy shocklets in compressible turbulence [5]. An other feature of the compressible component of the compressible energy is that is of the same order of magnitude as the solenoidal component at small scales and high wave numbers. The kinetic energy spectra of the Eulerian computation does not reflect this behavior to the same extend at small scales while it reproduces the result of the kinetic energies at large scales and small wave numbers. This is

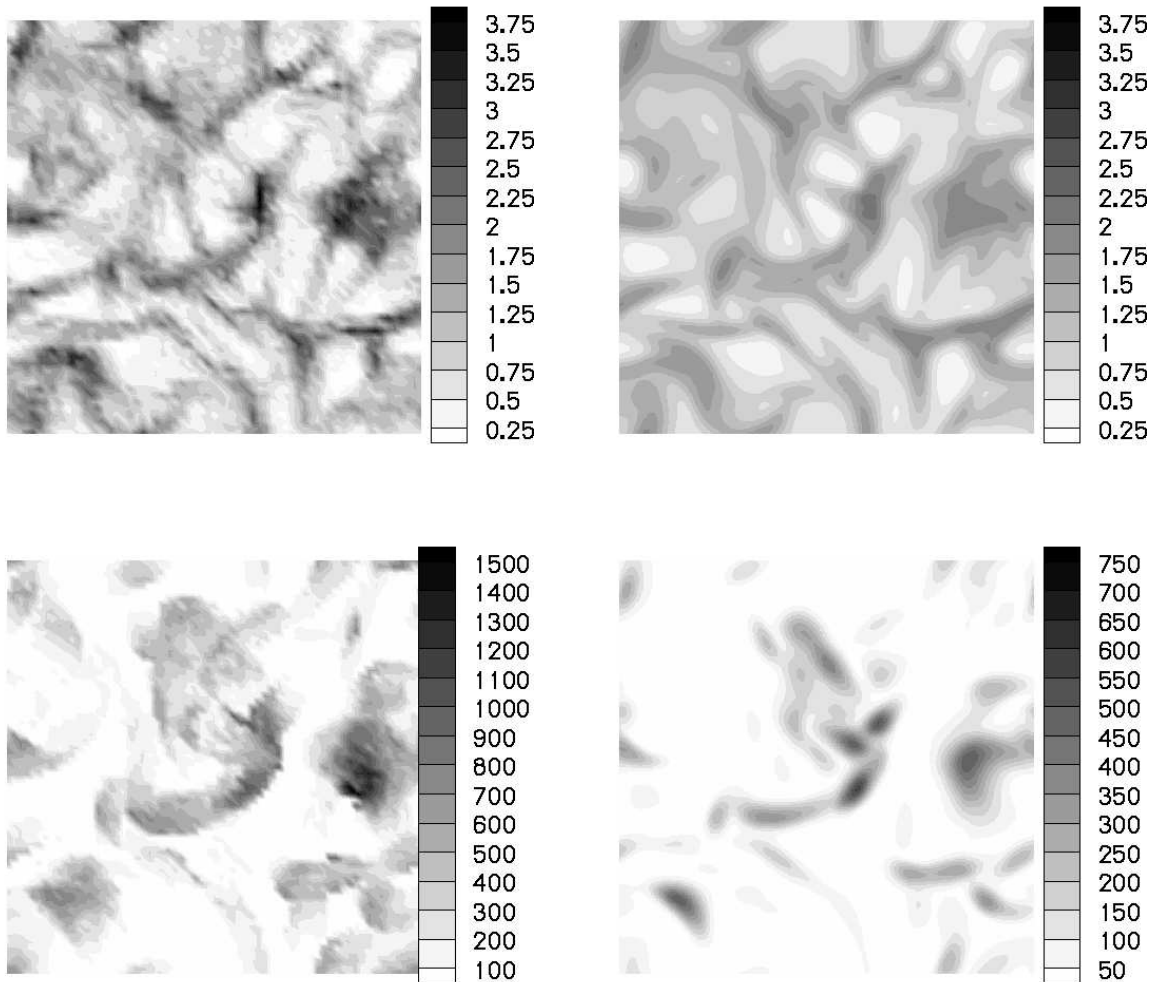


Figure 3: Comparison of the normalized droplet number ($\check{n}_p / \langle \check{n}_p \rangle$, upper graphs) and of the RUM Energy ($\delta\check{\theta}_p$, lower graphs) in the Lagrangian computation (left graphs, resolution 64^3) and the Eulerian computation (right graphs, resolution 128^3) after about one particle relaxation time ($t=10.8$). The cut plane has been defined a $z = 0$.

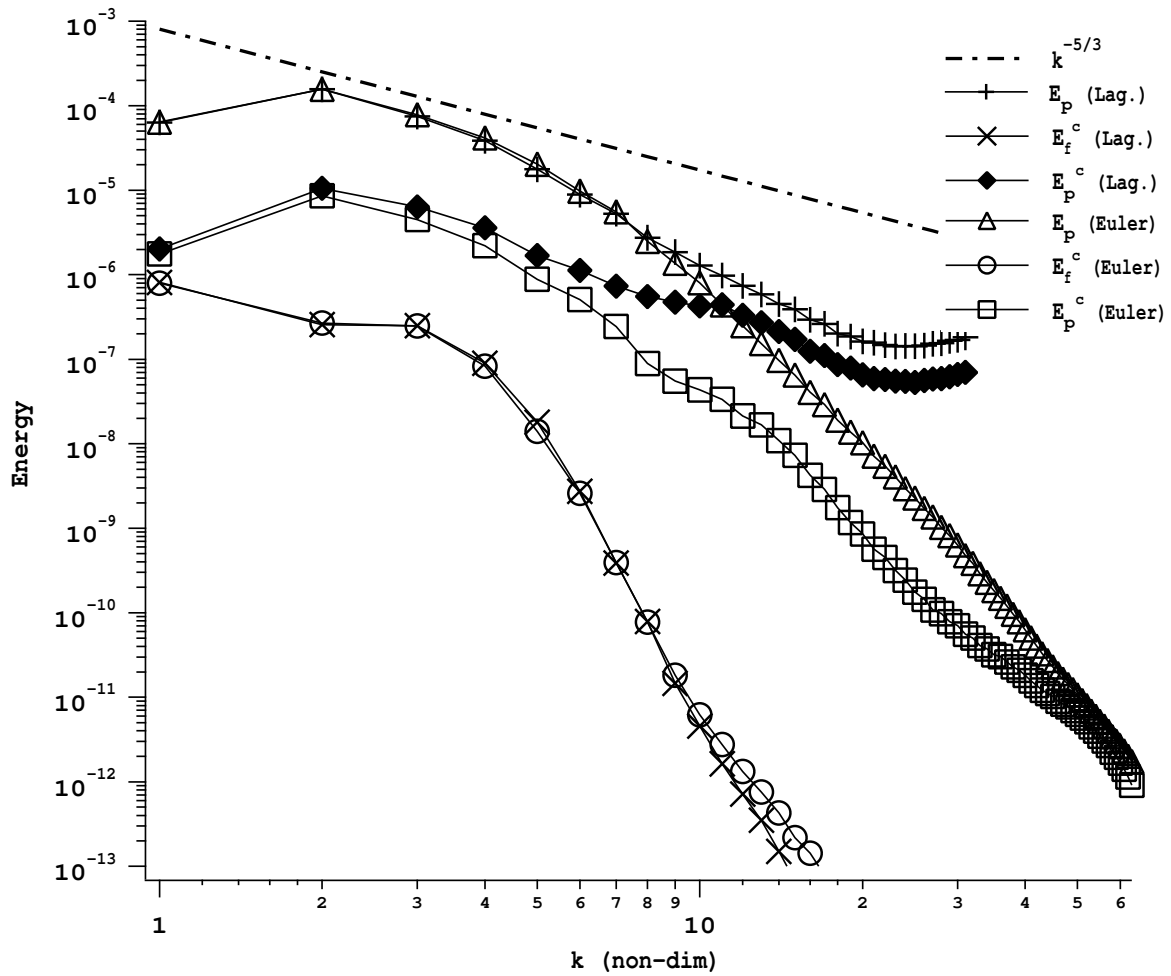


Figure 4: Comparison of Lagrangian and Eulerian kinetic energy spectra at $t=10.8$.

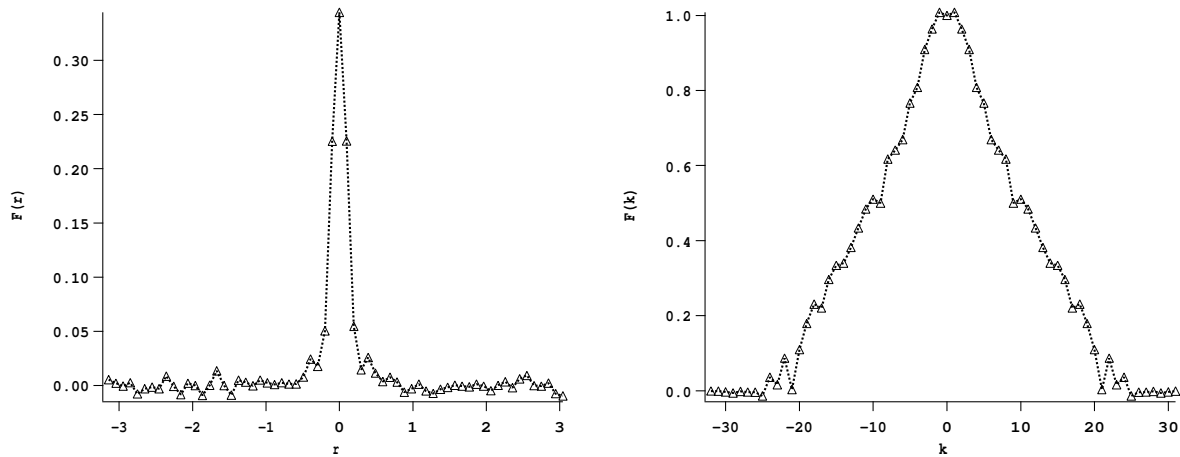


Figure 5: Filtering Kernel obtained by backward convolution between the Lagrangian number density field and the Eulerian number density field with a subgrid Pressure term. The left graph shows the spatial filter and the right graph shows the spectral filter.

at least partially due to the bulk viscosity operator introduced heuristically to make the computation possible.

7.4 Filtering Kernel

In the present case the unfiltered number density field is not available from the Eulerian computation. Therefore the equivalent Lagrangian number density field is used to obtain the filter kernel. The filter kernel is displayed in fig.5. Since the filter is considered isotropic in space, averaging over the different directions was performed and only the one dimensional kernel is retained. The figure shows that the convolution kernel averages the Lagrangian number density field a little more than the neighboring grid cells. If interpreting this graph, one has to keep in mind that the Lagrangian number density was already volume filtered to obtain a continuous field.

7.5 Comparison of filtered spectra

Fig. 6 shows the spectra of total and compressible kinetic energies of the Lagrangian simulation, of the filtered Lagrangian simulation using the filter described above and the Eulerian simulation. It shows that the spectrum obtained from the favre filtered Lagrangian results exhibits the same qualitative behavior as the spectra from the predictions of the Eulerian simulation. We conclude therefore that the filtering interpretation is consistent.

8 Conclusion and perspectives

The presented study shows the capacity of Eulerian formalism to capture the dynamics of particles at large scales even in the vicinity of unity Stokes numbers. Simulations were performed at very small turbulent Reynolds numbers since simulations with higher Reynolds numbers of the carrier phase showed deficiencies in the spatial resolutions of the dispersed phase. Therefore tests have to be extended to higher Reynolds numbers and it would be interesting to develop a subgrid model for the dispersed phase. This would lead to Large Eddy Simulations in an Eulerian framework which are very interesting for the unsteady computations of industrial applications with a high number of particles or droplets.

Eventually it is necessary to quantify the capacity of such an approach in real geometries other than the synthetic case of boxes with periodic boundary conditions. Possible configurations are particle

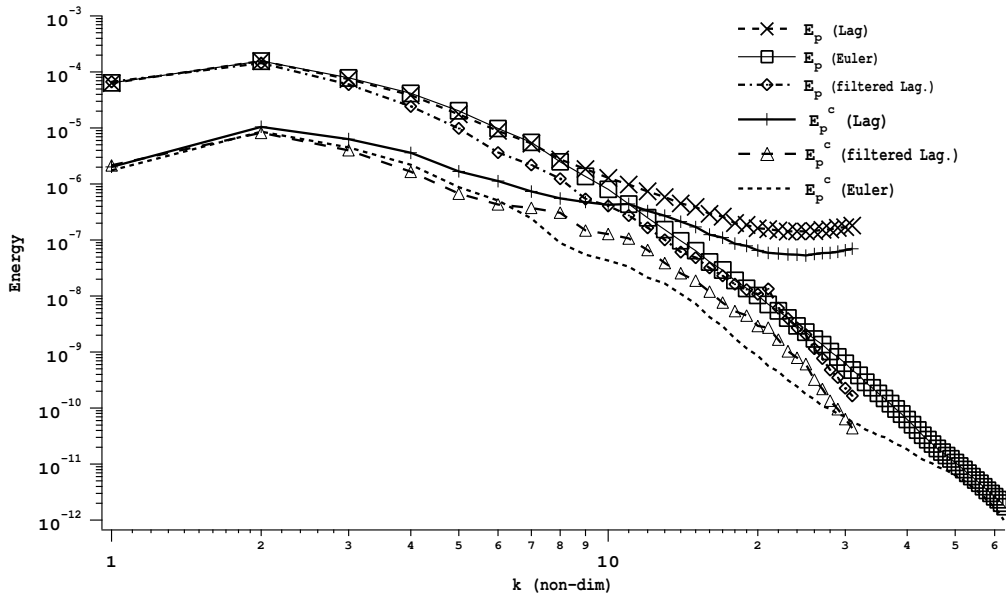


Figure 6: Total and compressible kinetic energy in the Lagrangian, filtered Lagrangian and Eulerian computation.

laden jets or particle laden channel flow with and without collisions. Those could be than be compared to Eulerian-Lagrangian simulations [18] and experiments [11] and show if the Eulerian-Eulerian approach has the same amount of mesoscopic velocity and RUM in wall bounded flows.

Acknowledgments

Numerical computation of the Eulerian simulations were performed on the COMPAQ supercomputers of CEA and CERFACS. Numerical solutions on large grids (192^3 , 256^3) were performed on SGI ORIGIN 3800 at CINES in the framework of the EXTREME COMPUTING FOR TURBULENT COMBUSTION program using up to 128 processors. The Lagrangian reference solution was obtained with numerical simulations performed at computing center IDRIS using the Eulerian-Lagrangian version of *NTMIX* in the *Ecoulements Reactifs Diphasiques: Simulations Directes et aux Grandes Echelles* project.

Financial support for this work was received from the European Community via the STOPP research training network.

References

- [1] S. Chapman and T.G. Cowling. *The Mathematical Theory of Non-Uniform Gases*. Cambridge University Press, cambridge mathematical library edition, 1939 (digital reprint 1999).
- [2] O.A. Druzhini and S. Elghobashi. Direct numerical simulations of bubble-laden turbulent flows using the two-fluid formulation. *Physics of Fluids*, 10(3):685–697, 1998.
- [3] O.A. Druzhini and S. Elghobashi. On the decay rate of isotropic turbulence laden with microparticles. *Physics of Fluids*, 11(3):602–610, 1999.
- [4] S. Elghobashi and G.C. Truesdell. Direct simulation of particle dispersion in a decaying isotropic turbulence. *Journal of Fluid Dynamics*, 242:655–700, 1992.

- [5] G. Erlebacher, M.Y.Hussaini, and C.G. Speziale T.A. Zang. Torward the large eddy simulation of compressible turbulent flows. *Icase*, 90-76:1–43, 1990.
- [6] P. Février. Etude numerique des effets de concentration preferentielle et de correlation spatiale entre vitesses des particules solides en turbulence homogene isotrope stationaire, phd thesis, inp toulouse,france 2000, 2000.
- [7] P. Février, O. Simonin, and K. D. Squires. Partitioning of particle velocities in two-phase turbulent flows into a continous field and a quasi-brownian distribution: theoretical formalism and numerical study. *submitted to Journal of Fluid Mechanics*, 2003.
- [8] J.O. Hirschfelder, C.F. Curtis, and R.B. Bird. *Molecular Theory of Gases and Liquids*. John Wiley & Sons, 1954 edition, 1954.
- [9] A. Kaufmann. Towards eulerian-eulerian large eddy simulation of reactive two-phase flows, phd thesis, inp toulouse,france 2004, 2004.
- [10] A. Kaufmann, J. Helie, Simonin O., and Poinso T. Comparison between lagrangian and eulerian particle simulations coupled with dns of homogeneous isotropic decaying turbulence. Estonian Akademie of Science, 2003.
- [11] D.A. Khalitov and E.K. Longmire. Effect of particle size on velocity correlations in turbulent channel flow. In *FEDSM03-45730*, 2003.
- [12] R.H. Kraichnan. An alomost markovian galilean-invariant turbulence model. *Journal of Fluid Mechanics*, 47:513, 1971.
- [13] T. Passot and A. Pouquet. Numerical simulation of compressible homogeneous flow in the turbulent regime. *Journal of Fluid Mechanics*, 181:441–466, 1987.
- [14] M.W. Reeks. On a kinetic equation fo the transport of particles in turbulent flows. *Physics of Fluids A*, 3(3):446–456, 1991.
- [15] O. Simonin. Combustion and turbulence in two phase flows. Lecture Series 1996-02, von Karman Institute for Fluid Dynamics, 1996.
- [16] O. Simonin, P. Février, and J. Laviéville. On the spatial distribution of heavy particle velocities in turbulent flow: from continous field to particulate choas. *Journal of Turbulence*, 3:040, 2002.
- [17] W.H. Snyder and J.L. Lumley. Some measurements of particle velocity autocorrelation functions in a turbulent flow. *Journal of Fluid Mechanics*, 48, part 1:41–71, 1970.
- [18] M.W. Vance, K. Squires, and O. Simonin. Properties of the particle field in gas-solid turbulent channel flow. In *5th International Conference on Multiphase Flow, Japan*, page Paper No. 530, 2004.
- [19] P.K. Yeung and Pope S.B. An algorithm for tracking fluid particles in numerical simulations of homogeneous turbulence. *Journal of Computational Physics*, 79:373–416, 1988.